4798 *Biochemistry* **2009,** *48,* 4798–4807
DOI: 10.1021/bi9004478

BIOCHEMISTRY
including biophysical chemistry & molecular biology
Article

Purification and Partial Characterization of a Lutein-Binding Protein from Human Retina[†]

Prakash Bhosale,[‡] Binxing Li,[‡] Mohsen Sharifzadeh,[§] Werner Gellermann,[§] Jeanne M. Frederick,[‡] Kozo Tsuchida,[∥] and Paul S. Bernstein*[,‡]

[‡]*Department of Ophthalmology and Visual Sciences, Moran Eye Center, University of Utah School of Medicine, Salt Lake City, Utah 84132,* [§]*Department of Physics, University of Utah, Salt Lake City, Utah 84112, and* [∥]*Division of Radiological Protection, National Institute of Infectious Diseases, Tokyo, Japan*

Received March 14, 2009; Revised Manuscript Received April 28, 2009

ABSTRACT: Dietary intake of lutein and zeaxanthin appears to be advantageous for protecting human retinal and macular tissues from degenerative disorders such as age-related macular degeneration. Selective concentration of just two of the many dietary carotenoids suggests that uptake and transport of these xanthophyll carotenoids into the human foveal region are mediated by specific xanthophyll-binding proteins such as GSTP1 which has previously been identified as the zeaxanthin-binding protein of the primate macula. Here, a membrane-associated human retinal lutein-binding protein (HR-LBP) was purified from human peripheral retina using ion-exchange chromatography followed by size-exclusion chromatography. After attaining 83-fold enrichment of HR-LBP, this protein exhibited a significant bathochromic shift of ~90 nm in association with lutein, and equilibrium binding studies demonstrated saturable, specific binding toward lutein with a K_D of 0.45 μM. Examination for cross-reactivity with antibodies raised against known lutein-binding proteins from other organisms revealed consistent labeling of a major protein band of purified HR-LBP at ~29 kDa with an antibody raised against silkworm (*Bombyx mori*) carotenoid-binding protein (CBP), a member of steroidogenic acute regulatory (StAR) protein family with significant homology to many human StAR proteins. Immunolocalization with antibodies directed against either CBP or GSTP1 showed specific labeling of rod and cone inner segments, especially in the mitochondria-rich ellipsoid region. There was also strong labeling of the outer plexiform (Henle fiber) layer with anti-GSTP1. Such localizations compare favorably with the distribution of macular carotenoids as revealed by resonance Raman microscopy. Our results suggest that HR-LBP may facilitate lutein's localization to a region of the cell subject to considerable oxidative stress.

The macula of the human eye is the cone-rich region of the retina responsible for high acuity vision necessary for reading, driving, and recognizing faces. Damage to this area of the retina frequently occurs in age-related macular degeneration (AMD),[1] the leading cause of irreversible blindness in the elderly in the developed world (*1*−*4*). While various animals have similar specialized regions for higher acuity vision such as the area centralis in some mammals and foveae in some birds, the human macula has unique features not found in any other animals outside of fellow primates (*5*−*11*). This uniqueness is emphasized by the formal anatomical name of the primate macula, the *macula lutea*. This "yellow spot" has long been known by anatomists to denote the center of the human macula. Wald characterized the macular pigment spectroscopically and determined that it was likely to be a xanthophyll carotenoid (*12*, *13*). Several decades later, Bone and Landrum demonstrated that the macular pigment was composed of a mixture of two dietary carotenoids, (3*R*,3′*R*,6′*R*)-lutein and (3*R*,3′*R*)-zeaxanthin, as well as a nondietary metabolite (3*R*,3′*S*-*meso*)-zeaxanthin (*14*). More recently, 3′-oxolutein, 3′-epilutein, and 3′-methoxyzeaxanthin were also identified as other important nondietary metabolites in the human macula (*10*, *11*, *14*, *15*).

At the center of the *macula lutea*, the inner retina thins due to the absence of the ganglion cell layer which is pushed eccentrically, leaving the cone axon layer (the Henle fiber layer) lining the foveal pit (*16*−*19*). The concentration of the macular carotenoids

[†]This work was supported by National Institutes of Health Grants EY-11600 and EY-014800-039003 (NEI core grant), by center grants of the Foundation Fighting Blindness, Inc., to the University of Utah, by an unrestricted grant to the Department of Ophthalmology at the University of Utah from Research to Prevent Blindness (RPB, New York, NY), and by Kemin Health (Des Moines, IA). K.T. was supported by the Teimei Empress and Futaba Memorial Foundations.

*To whom correspondence should be addressed. Tel: 801-581-6078. Fax: 801-581-3357. E-mail: paul.bernstein@hsc.utah.edu.

[1]AMD, age-related macular degeneration; CBP, silkworm carotenoid-binding protein; CHAPS, 3-[(3-cholamidopropyl)dimethylammonio]-1-propanesulfonate; CL-LBP, chicken liver lutein-binding protein; CRALBP, cellular retinaldehyde-binding protein; FITC, fluorescein isothiocyanate; GSTP1, glutathione *S*-transferase *pi* isoform; HPLC, high-performance liquid chromatography; HR-LBP, human retinal lutein-binding protein; HSA, human serum albumin; IEF, isoelectric focusing; MES, 4-morpholineethanesulfonic acid; MLN64, metastatic lymph node 64; PDI, protein disulfide isomerase; QL-LBP, quail liver lutein-binding protein; RPE, retinal pigment epithelium; RRI, resonance Raman imaging; StAR, steroidogenic acute regulatory; THF, tetrahydrofuran.

 Published on Web 04/29/2009

in the Henle fiber layer of the fovea is extraordinarily high, estimated at greater than 1 mM in many humans (*18*−*22*). This is by far the highest concentration of carotenoids anywhere in the human body, rivaled only by the *corpus luteum* of the ovary (*23*). The concentration of carotenoids decreases dramatically with increasing distance from the fovea, falling greater than 100-fold over a distance of just a few millimeters (*17*−*22*, *24*, *25*). Cross-sectionally, the highest levels of the macular carotenoids are in the inner and outer plexiform layers, with relatively low levels in the photoreceptor outer segments (*22*). In addition to spatial specificity, there is also remarkable chemical specificity of uptake into the human macula. In the fovea, the ratio of (3*R*,3′*R*,6′*R*)-lutein to (3*R*,3′*R*)-zeaxanthin to (3*R*,3′*S-meso*)-zeaxanthin is 1:1:1, while in the peripheral retina, lutein predominates over the zeaxanthins by a 3:1 ratio (*18*−*21*, *26*). Other common dietary carotenoids such as lycopene, carotenes, and cryptoxanthin cannot be converted to lutein or zeaxanthin in humans and are completely excluded from the human retina, yet they are found in abundance in serum, skin, and adjacent ocular tissues such as the retinal pigment epithelium (RPE) and the ciliary body (*10*).

Whenever a biological tissue exhibits chemical and spatial selectivity of uptake of a molecule, it is highly likely that this phenomenon is mediated by specific binding proteins (*27*). In the case of the macular carotenoids, this is further emphasized by the saturation effects often observed in dietary supplementation studies (nonresponders) and the difficulty of depleting macular pigment through dietary restrictions (*28*−*30*). In the plant and invertebrate world, numerous specific carotenoid-binding proteins have been purified and characterized from organisms as diverse as maize, bacteria, algae, lobsters, and silkworms (*31*−*35*). By contrast, much less is known about specific carotenoid-binding proteins in vertebrates. Various serum lipoproteins and their receptors appear to be involved in carotenoid transport and uptake (*36*, *37*), but specificity is not particularly high. In vertebrate tissues, polymeric structural proteins such as actin and tubulin appear to be sites for relatively low affinity binding of xanthophyll carotenoids (*38*, *39*). In 2004, we reported that the *pi* isoform of glutathione *S*-transferase (GSTP1) is the specific zeaxanthin-binding protein in the human macula (*27*). The protein copurifies with macular zeaxanthin, has the same spectral properties as the macular pigment *in vivo*, and is spatially localized to the inner and outer plexiform layers of the fovea, and the recombinant protein specifically binds the two macular forms of zeaxanthin with high affinity (*27*). In this study, we now report the initial purification and characterization of a comparable human retinal lutein-binding protein (HR-LBP), and we compare its immunolocalization to that of GSTP1 in monkey retina.

EXPERIMENTAL PROCEDURES

Purification of Human Retinal Lutein-Binding Protein (HR-LBP). Human donor eyecups were generously donated by the Utah Lions Eye Bank after corneas had been harvested for transplantation. All eyecups were kept on ice, and tissues were generally dissected and frozen within 24 h of death. After removing the vitreous and confirming the absence of significant visible pathology such as drusen, hemorrhage, or scarring, the macula was identified and excised with a 4 mm circular trephine. The remaining peripheral retina was then separated from the underlying retinal pigment epithelium (RPE) and stored separately.

In a typical preparation of HR-LBP, 16 thawed human peripheral retinas were homogenized on ice in 5 mL of a cell-lysing solution containing protease inhibitors (Roche Diagnostics, Mannheim, Germany) in 20 mM Tris buffer (pH 7.4) supplemented with 1 mM $CaCl_2$, 2 mM $MgCl_2$, and 15% (w/v) sucrose. Sucrose density gradient (5−50% w/v) centrifugation at 5000 rpm for 60 min at 2 °C resulted in a low-density yellow-colored fraction containing xanthophyll-binding proteins. The yellow fraction was then diluted with 20 mM Tris buffer (pH 7.4) to bring the sucrose concentration down to 5% (w/v). A high-speed ultracentrifugation of the low-speed supernatant was performed at 8 °C, and the yellow high-speed pellet was solubilized with brief sonication on ice into 500 μL of 25 mM 3-[(3-cholamidopropyl)dimethylammonio]-1-propanesulfonate (CHAPS) in 20 mM 4-morpholineethanesulfonic acid (MES) buffer (pH 5.5) followed by centrifugation at 100,000*g* for 60 min at 2 °C. The CHAPS-insoluble pellet was resolubilized into CHAPS/MES several more times followed by high-speed centrifugation as described above. The pale yellow CHAPS-solubilized supernatants were combined and concentrated to 500 μL using an Ultrafree centrifugal filtration system (Millipore, Woburn, MA; molecular mass cutoff 10 kDa).

Protein chromatography was performed on a BioLogic liquid chromatography system (Bio-Rad, Hercules, CA). Detergent-solubilized human macular membrane extracts were loaded immediately after preparation onto an Amersham Biosciences (Piscataway, NJ) Q anion-exchange column (7 × 35 mm, N $(CH_3)_3^+$ exchanging groups). Initial buffer conditions were 20 mM Tris buffer (pH 7.4) containing 8 mM CHAPS followed by a linear gradient run at 1.0 mL/min at 4 °C from 0 to 1 M NaCl over 20 min. At later purification stages, cation-exchange chromatography was performed on an Amersham Biosciences S column (7 × 35 mm, SO_3^- exchanging groups). Initial buffer conditions were 20 mM MES buffer containing 8 mM CHAPS at pH 5.5 run at 0.5 mL/min at 4 °C for 15 min, followed by a linear gradient from 0 to 1 M NaCl over 15 min. Size-exclusion chromatography was then performed using a silica gel filtration column (BIOSEP-SEC-S 3000 PEEK, 300 × 7.80 mm, separation range 5−700 kDa; Phenomenex, Torrance, CA) to differentiate proteins based on molecular mass. Concentrated fractions (up to 200 μL) from the ion-exchange columns were loaded onto the gel filtration column, and 50 mM sodium phosphate buffer (pH 7.0) containing 8 mM CHAPS was used as the eluant at a 0.5 mL/min flow rate. At all stages of chromatographic purification, the eluates were monitored by a UV6000 photodiode array spectrophotometer equipped with a high-sensitivity 50 mm path length light-pipe flow cell with an internal volume of 10 μL (Thermo Fisher, San Jose, CA), and 300 μL fractions were collected. The fractions of interest containing proteins associated with endogenous xanthophyll carotenoids exhibited strong 280 nm protein absorbance and prominent triple peak vibronic structure typical of most carotenoids centered at ~460 or ~540 nm.

Carotenoid Extraction and High-Performance Liquid Chromatography (HPLC). Fifty microliters of purified fractions at each stage of column chromatography was treated with 100 μL of methanol to disrupt ligand−protein associations, and they were then extracted into 200 μL of hexane. Phase separation was promoted by addition of 20 μL of saturated sodium chloride. The organic extracts were dried by vacuum evaporation in a Speedvac Plus (SC110; Savant, Cambridge, MA) and redissolved in 1 mL of HPLC mobile phase [hexane:dichloromethane:

methanol:*N*,*N*-diisopropylethylamine (80:19.2:0.7:0.1 v/v)]. HPLC separation was carried out at a flow rate of 1.0 mL/min on a cyano column (Microsorb 25 cm length × 4.6 mm i.d.; Varian Inc., Palo Alto, CA). The column was maintained at room temperature, and the HPLC detector was operated at 450 nm. Peak identities were confirmed by photodiode array spectra and by co-elution with authentic standards as necessary. Peak areas were integrated and quantified with an external standardization curve.

Two-Dimensional Isoelectric Focusing and Electrophoresis. Isoelectric focusing (IEF) separations were done using precast immobilized pH gradient (IPG) gel strips (pH 5−8, strip length 11 cm; Bio-Rad). The IPG strips were rehydrated overnight in trays loaded with the protein samples in the manufacturer's sample buffer. Isoelectric focusing was performed in a Bio-Rad Protean IEF cell unit at 20 °C, with a maximum current of 50 μA/strip. The end voltage for the IEF run was 8000 V. The strips were equilibrated with buffers containing dithiothreitol and iodoacetamide. Following SDS−PAGE on a 1 mm thick 4−20% gradient Tris-HCl gel, protein spots were stained with fluorescent Sypro Ruby protein stain (Bio-Rad). Gels were then visualized and documented using a Bio-Rad UV light source.

Western Blots. Protein samples were separated on 4−15% gradient SDS−PAGE and transferred to 0.45 μm nitrocellulose membranes using a Bio-Rad trans-blot apparatus at 100 V for 2 h. Nonspecific binding was blocked by immersing the membrane in 5% (w/v) nonfat dried milk in 0.01% (v/v) Tween 20 in phosphate-buffered saline (PBS) for 1 h at room temperature on an orbital shaker. The membrane was briefly rinsed with two changes of wash buffer and incubated with primary antibody overnight. The antibody to silkworm (*Bombyx mori*) carotenoid-binding protein (CBP) diluted 1:1000 was raised in the laboratory of Dr. Kozo Tsuchida, Division of Radiological Protection, National Institute of Infectious Diseases, Tokyo, Japan (*34*), and the antibody to actin (1:500 dilution) came from Sigma-Aldrich (St. Louis, MO). After two changes of wash buffer, peroxidase-conjugated affinity-purified secondary antibody was diluted in the PBS and incubated for 1 h (1:1000 goat anti-rabbit IgG(H + L)-HRP-conjugated antibody from Alpha Diagnostics International, San Antonio, TX). The membranes were developed using ECL Plus Western blot detection reagents (Amersham Biosciences, Piscataway, NJ).

Carotenoid-Binding Assay with HR-LBP. Synthetic (3*R*,3′*R*)-zeaxanthin, (3*R*,3′*S-meso*)-zeaxanthin, and 3′-oxolutein were gifts from DSM Nutritional Products (Kaiseraugst, Switzerland), and (3*R*,3′*R*,6′*R*)-lutein prepared from marigold flowers was a gift from Kemin Health (Des Moines, IA). Ocular xanthophyll-binding proteins generally require CHAPS detergent to maintain solubility and stability during purification (*27*), and the CHAPS detergent also aids in solubilizing the xanthophyll carotenoid ligands; therefore, all carotenoid-binding experiments were done in the presence of identical concentrations of CHAPS. Ten microliters of concentrated carotenoids dissolved in tetrahydrofuran (THF) was added to 490 μL of 50 mM Tris−CHAPS (8 mM) buffer containing 1 μg of HR-LBP as estimated by a Bradford protein assay kit (Bio-Rad). After brief mixing, the solution was incubated overnight (16 h) at 4 °C. Unbound carotenoids were removed by four cycles of gentle extraction with 200 μL of hexane, followed by centrifugation for 5 min in a microcentrifuge. Residual hexane was removed from the extracted sample under a stream of argon or under vacuum, and then HPLC carotenoid analysis was performed on the samples. Computerized nonlinear regression analyses of binding parameters using one and two binding-site models were performed using the PRISM version 3.0 package from Graph Pad (La Jolla, CA). All binding curves and calculations were corrected for nonspecific binding by subtracting parallel incubations in which protein had been omitted.

Immunohistochemistry. Confocal microscope images derive from two *Macaca fascicularis* monkeys, aged 3 and 9 years old, whose eyes had been perfused with 4% paraformaldehyde in 0.1 M phosphate buffer for 15−20 min at the time of sacrifice (provided by Dr. Alessandra Angelucci at the Moran Eye Center). After removal of the anterior segment and vitreous, each eyecup was rinsed and cryoprotected overnight in 0.1 M phosphate buffer (pH 7.4) containing 30% sucrose. A rectangular piece of retina centered approximately on the fovea was isolated, embedded, and frozen. Cryosections 12 μm thick were cut, rinsed in 0.1 M phosphate buffer containing 0.1% Triton X-100 (PBT), and blocked for 1 h using 10% normal donkey serum in PBT. Antibodies to GSTP1 (Alpha Diagnostic International, San Antonio, TX; 1:1000 dilution) or silkworm (*B. mori*) carotenoid-binding protein (CBP) (raised in the laboratory of Dr. Kozo Tsuchida, Division of Radiological Protection, National Institute of Infectious Diseases, Tokyo, Japan; 1:1000 dilution (*34*)) were coincubated overnight at 4 °C with cone arrestin monoclonal antibody (mAb 7G6 from Dr. Peter R. MacLeish, Morehouse School of Medicine, Atlanta, GA; 1:1000 dilution). After rinsing in PBT three times for 10 min, rhodamine- and fluorescein isothiocyanate- (FITC-) conjugated secondary antibodies (Jackson ImmunoResearch Laboratories, West Grove, PA; each 1:200 dilution) were applied for 2 h at room temperature. Immunolocalization was imaged using a Zeiss LSM 510 confocal microscope set to an optical slice of <0.9 μm. Control sections, in which incubation in primary antibodies was omitted, were processed in parallel and revealed that immunoreactivity of the retina was negative and that the signal of the RPE was nonspecific.

To determine whether lutein- and zeaxanthin-binding proteins were overlapping in distribution, monkey sections were blocked for 1 h using 10% donkey serum in PBT and incubated overnight with anti-CBP (1:1000 dilution) at 4 °C. After rinsing in PBT as above, rhodamine-conjugated donkey anti-rabbit secondary antibody was applied for 1 h at room temperature. Because the antibodies directed toward both binding proteins were polyclonal and were raised in rabbit, the sections were washed thoroughly in PBT and reblocked using 10% goat serum. Anti-GSTP1 (1:1000 dilution) was applied to the retina sections for 1 h. After rinsing, the sections were incubated in FITC-conjugated goat anti-rabbit secondary antibody for 1 h, rinsed, and imaged as described above. Similarly, to determine whether lutein- or zeaxanthin-binding proteins were found in Müller glia, CBP or GSTP1 labeling was followed by that of a polyclonal antibody to cellular retinaldehyde-binding protein (CRALBP) (supplied by Dr. Jack Saari, University of Washington; 1:1000 dilution).

Resonance Raman Imaging. Monkey retinal tissue sections were also imaged using a resonance Raman imaging (RRI) microscope constructed using a design similar to our *in vivo* resonance Raman imaging instrument (*40*). A schematic of the RRI microscope is shown in Figure 11. Excitation light from a 488 nm argon laser (National Laser, Salt Lake City, UT; power 0.5 mW, exposure time 600 s) was routed onto the sample with an optical fiber, a collimating lens, L1, a laser line filter, F1, an achromatic beam expander, L2, a holographic beam splitter,

Table 1: Purification of Human Retinal Lutein-Binding Protein (HR-LBP)

step	column	protein content in preparations (μg/μL)	$A_{537/280}$	lutein (% of total carotenoids)	purification (x-fold)
1	extract[a]	0.9	0.01	75	1
2	Q (unbound)	0.13	0.12	82	12
3	S (bound)	0.06	0.71	87	71
4	silica gel	0.003	0.83	94	83

[a] Extract represents the preparation after sucrose density gradient ultracentrifugation.

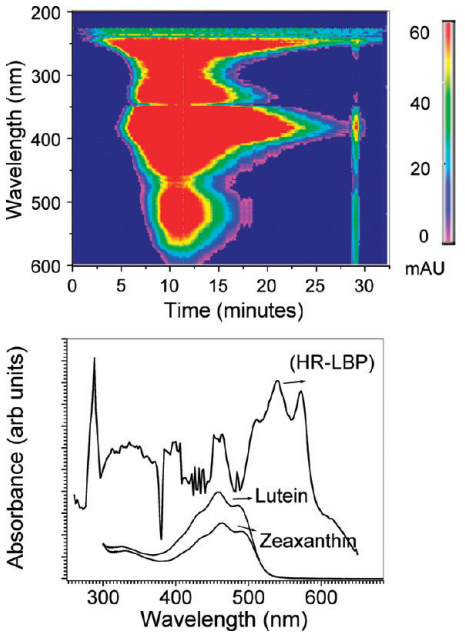

FIGURE 1: Elution pattern of HR-LBP on a silica gel size-exclusion chromatographic column. Contour view of the online photodiode array scans performed at 0.5 s intervals during the chromatographic purification of HR-LBP (upper panel). Absorbance spectrum of purified HR-LBP eluting from the silica gel column at 11 min compared with that of (3*R*,3′*R*)-zeaxanthin and (3*R*,3′*R*,6′*R*)-lutein standards dissolved in THF (lower panel). There is a bathochromic shift of the absorbance peaks of HR-LBP (507, 537, 589 nm) relative to zeaxanthin (425, 456, 478 nm) and lutein (425, 450, 476 nm).

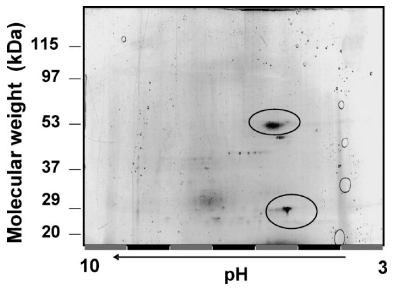

FIGURE 2: Two-dimensional IEF and SDS−PAGE of HR-LBP. An aliquot of highly purified HR-LBP was subjected to isoelectric focusing and SDS−PAGE analysis according to procedures detailed in the Experimental Procedures section. Protein spots were stained with fluorescent Sypro Ruby protein stain and then visualized using a UV light source.

HBS, and an aperture interfaced to a microscope objective. The laser excitation spot projected onto the sample was ~100 μm diameter and has an intermediate focus at the position of the aperture. Laser speckle was effectively removed by mechanically shaking the light delivery fiber of the excitation laser beam. This generates a spatially homogeneous laser excitation spot via fiber mode mixing. The light emitted from the excited region of the retina was collimated and imaged with a 50 mm achromat onto the 512 × 512 pixel array of a CCD camera (Model ST-9 XE; Santa Barbara Instrument Group, Inc., Santa Barbara, CA). The instrument is interfaced to a computer that controls a mechanical shutter and acquires data via camera-manufacturer-supplied software. For data analysis, the pixel intensity maps are processed with image processing software (The MathWorks, Inc., Natick, MA).

Resonance Raman images are derived from two measurements taken with a narrow-band tunable filter, F3 (transmission range 528 ± 1 nm), that is angle tuned to "on" and "off" Raman spectral positions (*40*). The light returned from the sample is filtered to transmit only 528 nm light, which is the spectral position of the resonance Raman response of the 1525 cm^{-1} carbon−carbon double bond stretch vibration of carotenoids when excitation is at 488 nm. This is achieved with a combination of a narrow bandpass filter, a broad bandpass filter (transmission window 525 ± 15 nm), a notch filter, F2, and an aperture (diameter, ~1 mm), which limits any reflected excitation stray light to a small beam diameter with paraxial propagation. The section was then reimaged with F3 adjusted to an off-resonance position several nanometers away from 528 nm. Digital subtraction of the off-resonance image from the on-resonance image yields a specific image of carotenoid concentrations and distributions.

RESULTS

Purification of HR-LBP. We have previously reported the purification of the major zeaxanthin-binding protein from human macula and its identification as GSTP1 (*27*). Our strategy for the purification of the zeaxanthin-binding protein was to utilize the tissue with the highest endogenous zeaxanthin-to-protein ratio, the human macula, and to use photodiode array monitoring throughout the chromatographic purification process to maximize the ratio of macular pigment absorbance at ~460 nm to protein absorbance at 280 nm. We found that the zeaxanthin-binding protein from the human macula was membrane-associated, requiring detergent solubilization in CHAPS. The solubilized protein did not bind to moderately charged cation- or anion-exchange columns, indicating high relative hydrophobicity in a detergent environment. Subsequent gel filtration chromatography produced a zeaxanthin-rich band with one major protein spot on 2-D gels. Sequencing of this spot identified the protein as GSTP1, and recombinant GSTP1 exhibited the characteristics expected of a zeaxanthin-binding protein including specific high-affinity binding of (3*R*,3′*R*)-zeaxanthin and (3*R*,3′*S-meso*)-zeaxanthin, induced circular dichroism upon binding (3*R*,3′*S-meso*)-zeaxanthin, and prominent immunolocalization to the Henle fiber layer of the human macula.

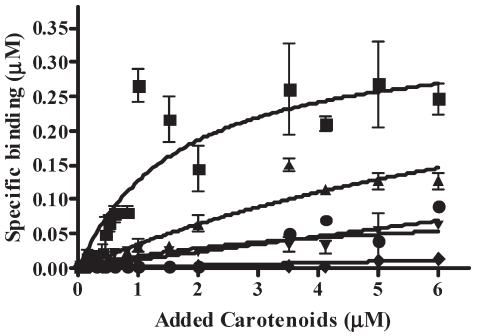

FIGURE 3: Binding studies of HR-LBP with retinal xanthophylls. Ten microliters of concentrated xanthophylls dissolved in THF was added to 490 μL of 50 mM Tris−CHAPS (8 mM) buffer containing 1 μg of HR-LBP. After brief mixing, the mixtures were incubated overnight (16 h) at 4 °C. Unbound carotenoids were removed by four cycles of extraction with 200 μL of hexane and analyzed by HPLC. [(■) (3*R*,3′*R*,6′*R*)-lutein, (●) 3-methoxyzeaxanthin, (▼) (3*R*,3′*R*)-zeaxanthin, (▲) (3*R*,3′*S-meso*)-zeaxanthin, and (♦) 3′-oxolutein.]

Table 2: Western Blot Specificity of Various Antibodies with Potential Lutein-Binding Proteins[a]

	antibodies				
protein	anti-CBP	anti-StAR1	anti-MLN64	anti-PDI	anti-HSA
CBP	+	+	−	−	−
StAR	+	+	+	−	−
HR-LBP	+	−	−	−	−
QL-LBP	+	+	−	−	−
CL-LBP	+	+	−	−	−
PDI	−	−	−	+	−
HSA	−	−	−	−	+

[a] Abbreviations: CBP, silkworm carotenoid-binding protein; StAR, steroidogenic acute regulatory protein mixture isolated from mouse adrenal gland; HR-LBP, human retinal lutein-binding protein; QL-LBP, quail liver lutein-binding protein; CL-LBP, chicken liver lutein-binding protein; PDI, protein disulfide isomerase; HSA, human serum albumin; anti-StAR1, an antibody to StAR1 protein; anti-MLN64, an antibody to MLN64 (a StAR protein). Antibodies against StAR1 and MLN64 were from Affinity BioReagents (Golden, CO). Antibodies against PDI and HSA were from Sigma-Aldrich (St. Louis, MO).

During the purification of GSTP1, we noted the presence of another potential xanthophyll-binding protein also with a three-peak absorbance pattern typical of many xanthophyll carotenoids. In contrast to the macular zeaxanthin-binding protein, this membrane-associated protein bound to the cation-exchange column and exhibited a much larger bathochromic shift (~90 nm versus ~10 nm), properties very similar to our previously reported xanthophyll-binding protein isolated from quail liver (*35*). Carotenoid analysis of this second band indicated that it was enriched in lutein relative to zeaxanthin. The limited supply of human macular tissue made further characterization of this protein band challenging, so we turned to a more abundant lutein-rich tissue source, the human peripheral retina. As shown in Table 1, we achieved an 83-fold enrichment of HR-LBP as measured by the A_{537}/A_{280} ratio. In the most purified preparation, lutein accounted for 94% of the associated carotenoids with the other 6% consisting mainly of zeaxanthin and 3′-oxolutein. Photodiode array spectroscopy at the final chromatography step demonstrated a three-peak absorbance characteristic of lutein and zeaxanthin in organic solvents but bathochromically shifted ~90 nm to 537 nm (Figure 1). On 2-D gels there were two major spots at ~55 kDa and at ~29 kDa (Figure 2). Equilibrium

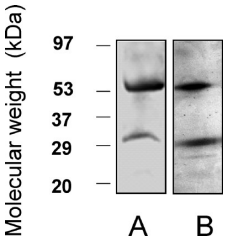

FIGURE 4: Western blot against highly purified HR-LBP with polyclonal antibody to the silkworm carotenoid-binding protein (CBP). The left lane (A) is a fluorescent Sypro Ruby protein stain of the purified protein, and the right lane (B) is the corresponding immunoblot run in parallel.

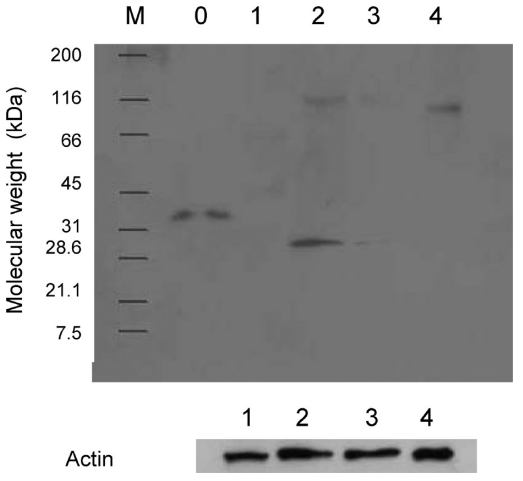

FIGURE 5: Western blot of CBP antibody against whole protein extracts. Lanes 1−4 were normalized against actin. Lane 0, purified carotenoid-binding protein from silkworm (note that a bubble artifact is present); lane 1, mouse retinal proteins; lane 2, human macular proteins; lane 3, human peripheral retinal proteins; lane 4, human retinal pigment epithelium (RPE) proteins. CBP has the expected molecular mass of ~34 kDa. There is strong labeling of a ~29 kDa band in human macula and a fainter band of the same molecular mass in human peripheral retina, consistent with the greater than 10-fold higher concentration of lutein in the macula versus the peripheral retina. Mouse retina and human RPE had no detectable labeling below 100 kDa.

binding studies on purified HR-LBP demonstrated saturable, specific, high-affinity binding toward lutein with a K_D of 0.45 μM, while all other xanthophylls found in the human retina in substantial quantities exhibited nonsaturable, low-affinity binding (Figure 3). This K_D is comparable to GSTP1's affinity for zeaxanthin (*27*) and is in the physiological range for serum carotenoid concentrations.

Western Blots of HR-LBP. Multiple attempts at mass spectral protein sequencing of purified HR-LBP from one- and two-dimensional gels proved unrevealing, perhaps due to the protein's hydrophobic nature or to posttranslational modificiations. Signals were weak, with detected sequences consisting primarily of well-known proteins such as human serum albumin (HSA) and protein disulfide isomerase (PDI) whose antibodies were unreactive with the purified protein and which failed to show labeling consistent with a xanthophyll-binding protein on immunohistochemistry. We therefore sought out an alternative approach to HR-LBP's identification by examining for cross-reactivity with antibodies raised against known lutein-binding proteins from other organisms. We obtained a highly specific polyclonal antibody to the silkworm (*B. mori*) carote-

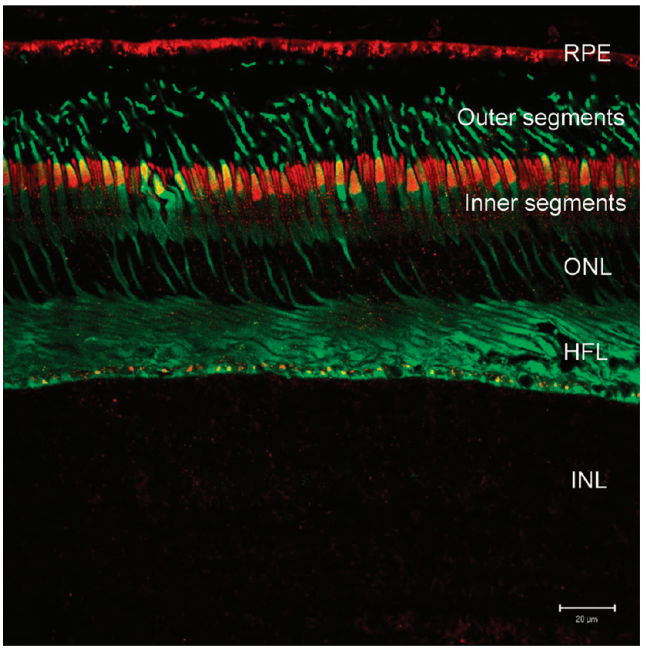

FIGURE 6: Immunolocalization with antibody to CBP in 9-year-old monkey macula near the optic nerve. Cones (green) are identified using the monoclonal antibody 7G6, which recognizes primate cone arrestin. Polyclonal anti-CBP antibody (red) labels specifically the ellipsoid regions of both rod and cone photoreceptors. Punctate label appearing in cone pedicles is considered to be nonspecific as it is unaffected by preabsorption of the antibody with purified protein. The red color of the RPE is due to nonspecific immunoreactivity and autofluorescence since it was still present when the primary antibody was omitted. Magnification bar = 20 μm for each of Figures 7−11. Abbreviations: RPE, retinal pigmented epithelium; ONL, outer nuclear layer; HFL, Henle fiber layer; INL, inner nuclear layer.

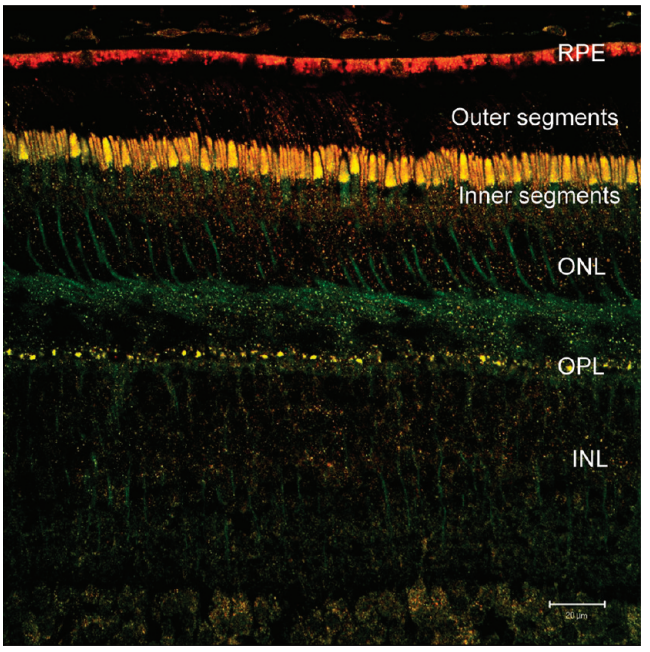

FIGURE 7: Colocalization of antibodies to CBP and GSTP1 in 9-year-old monkey macula near the optic nerve. Polyclonal antibodies against CBP (red) and GSTP1 (green) label all macular rods and cones. Labeling for GSTP1 appears prominently in the cone inner segments and, to a lesser extent, the cone axons of Henle's fiber layer. Colocalization with CBP (yellow) occurs predominantly in the photoreceptor ellipsoid regions. The red color of the RPE is due to nonspecific immunoreactivity and autofluorescence since it was still present when the primary antibody was omitted. Abbreviation: OPL, outer plexiform layer.

noid-binding protein (CBP) (*33*, *34*, *41*). This protein is essential for dietary uptake of lutein in this insect. It binds lutein specifically and with high affinity, and it is a member of the steroidogenic acute regulatory (StAR) protein family with significant homology to other human StAR proteins such as StAR1 and MLN64 (metastatic lymph node 64). As shown in Table 2 and Figure 4, the antibody against CBP reacted strongly with the upper and lower bands of HR-LBP and with the lutein-binding proteins isolated from quail liver (QL-LBP) and chicken liver (CL-LBP). It also reacted strongly with the original antigen and with an extract from mouse adrenal gland, a rich source of various mammalian StAR proteins (*42*). The antibody did not react with unrelated proteins such as albumin or protein disulfide isomerase. There are at least 15 StAR proteins in humans (*43*), and until recently, antibodies to just a few StAR proteins were commercially available. Antibodies to StAR1 and MLN64 reacted with adrenal extracts, but only the antibody against StAR1 reacted with various lutein-binding proteins including CBP, QL-LBP, and CL-LBP, but not HR-LBP. Quantitative Western blotting with the polyclonal antibody to CBP (MW 34 kDa) against crude protein extracts from human macula, human peripheral retina, human RPE/choroid, and mouse retina normalized to total actin demonstrated strong immunoreactivity of human macula and much weaker immunoreactivity of human peripheral retina at 29 kDa, consistent with the greater than 10-fold higher concentration of lutein in the macula versus the peripheral retina (Figure 5). No immunoreactivity was detected with mouse retina or human RPE/choroid in this molecular mass range. We did not observe immunoreactivity at ~55 kDa in these unpurified protein preparations, suggesting that HR-LBP may tend to dimerize when in a highly purified state or that an epitope reactive with anti-CBP antibody is masked in the crude protein preparations.

Immunohistochemistry with Antibodies against CBP and GSTP1. Immunohistochemistry was performed on frozen sections of two perfusion-fixed monkey maculas with identical results. The antibody directed against silkworm CBP labeled both rod and cone inner segments intensely, especially in the ellipsoid regions (Figure 6), while antibody directed against human StAR1 protein showed no retina labeling. Punctate regions of cone pedicles also appeared labeled with anti-CBP, but this was nonspecific because preabsorption of the anti-CBP antibody with the purified antigen eliminated immunoreactivity associated with rod and cone inner segments without affecting signal associated with the cone pedicles. Photoreceptor axons were only weakly labeled by anti-CBP, and there was virtually no labeling of the outer segments. With the antibody to GSTP1, there was a similar labeling pattern with the addition of specific labeling of the cone axons in the Henle fiber layer. Labeling intensity of photoreceptors with anti-GSTP1 was relatively weak near the optic nerve (Figure 7) but very robust near the fovea (Figures 8 and 9). Signal associated with the RPE was nonspecific, appearing with application of the secondary antibody along with some autofluorescent contribution. Gass and others have speculated that the macular pigment is localized to the foveal Müller cells rather than the photoreceptors (*44*), but double-labeling experiments with an antibody to cellular retinaldehyde-binding protein (CRALBP) provided by Dr. Jack Saari (University of Washington), a Müller cell-specific protein in the neural retina, demonstrated absence of colabeling with either

anti-CBP or anti-GSTP1 (Figure 10). Labeling intensity with either antibody was much lower in peripheral sections of monkey retina, and there was only diffuse nonspecific labeling in the retina of the mouse, an animal that does not accumulate significant levels of carotenoids in the eye (data not shown).

Resonance Raman Localization of Carotenoids in the Retina. In order to assess whether the localization of the antibodies to CBP and GSTP1 corresponded to the highest concentrations of macular carotenoids, we constructed an argon laser resonance Raman microscope (Figure 11) to image the carotenoids using the same principles we have developed for *in vivo* resonance Raman imaging of macular carotenoid distributions (*40*). Two sections of monkey retina were used, one in the parafoveal area on the slope of the foveal pit and one in the peripheral macula at about 3 mm eccentricity. The Raman image taken with 488 nm excitation of the parafovea showed intense signal from the outer plexiform layer corresponding to the cone axons of the Henle fiber layer and virtually no signal from all of the other layers (Figure 12). A similar, but much weaker Raman signal pattern was present in the more peripheral tissue section. Quantitative comparison of the parafovea with the more peripheral section indicated a 100-fold decline in signal intensity in the outer plexiform layer. The intense signal seen in the outer plexiform layer corresponded well with the labeling pattern seen with the antibody to GSTP1 and less well with the antibody to CBP which tends to label the inner segments predominantly. At the time of these experiments, we did not have access to 532 nm excitation in our apparatus, but we speculate that this wavelength may be more suitable for excitation of lutein bound to HR-LBP since it is the likely resonance wavelength for the bathochromically shifted complex.

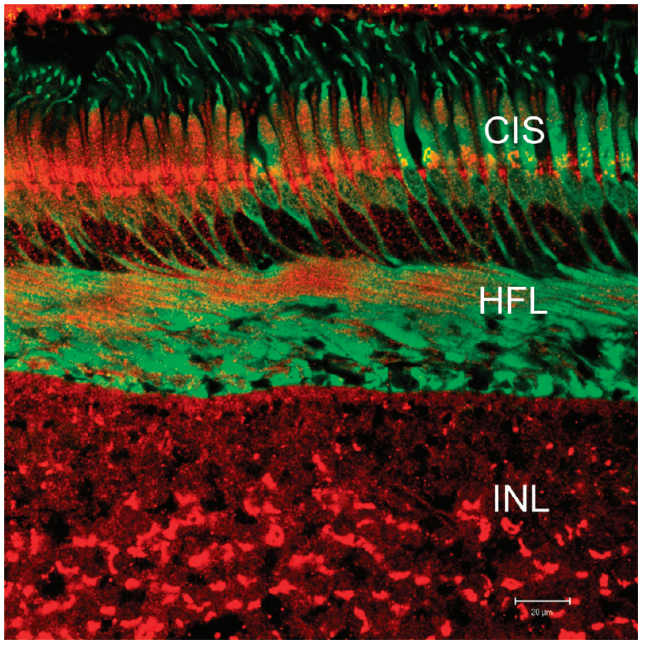

FIGURE 8: Immunolocalization with antibody to GSTP1 in parafovea of a 3-year-old monkey. Cones (green) are identified using the monoclonal antibody 7G6, which recognizes primate cone arrestin. Antibody directed against GSTP1 (red) labels intensely cone inner segments (CIS) and axons of the Henle fiber layer (HFL) in addition to perinuclear regions of horizontal, bipolar, and amacrine cells of the inner nuclear layer (INL).

DISCUSSION

Although carotenoids are exclusively synthesized by plants and microorganisms where they are typically employed for light harvesting and photoprotection, many invertebrates and vertebrates co-opt these common dietary constituents for their own physiological functions (*35*). Lobsters incorporate astaxanthin into a specific binding protein known as crustacyanin to color their shells (*45*), birds concentrate various xanthophyll carotenoids in egg yolks and feathers (*46*, *47*), and β-carotene is cleaved by specific enzymes to yield vitamin A (*36*, *48*, *49*). Recurrent in these processes is the involvement of specific proteins that mediate the tissue uptake, transport, stabilization, and metabolism of carotenoid compounds (*31*, *33*−*38*, *41*, *50*, *51*). Our laboratory has long focused on defining the proteins responsible for the highly specific deposition of lutein, zeaxanthin, and their metabolites in the human macula and peripheral retina where there is a wealth of evidence that they serve to protect against light-induced oxidative damage that may ultimately lead to visual loss from disorders such as age-related macular degeneration (*11*, *15*, *26*, *27*, *35*, *38*, *50*).

Initially, we demonstrated that retinal tubulin can serve as a high-capacity, low-affinity, relatively nonspecific site for carotenoid deposition in the human retina (*38*). Next, we were able to demonstrate that GSTP1 is a specific binding protein for the zeaxanthins found in the human macula (*27*). Later, we provided evidence for a lutein-binding protein with a large bathochromic shift in avian liver (*35*). Now, in this study we report the presence of a comparable lutein-binding protein in the human retina that fulfills many of the criteria expected of a specific lutein-binding protein including co-purification of the protein with endogenous lutein in a multistep biochemical purification, saturable and specific binding with exogenously added carotenoids, and spectral alterations characteristic of carotenoid−protein interactions (large bathochromic shifts and/or induced circular dichroism). Interestingly, the purified human retinal lutein-binding protein is strongly labeled by a polyclonal antibody raised against a lutein-specific silkworm carotenoid-binding protein (CBP),

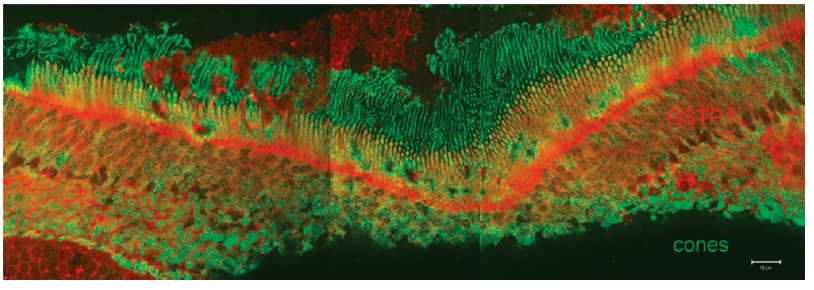

FIGURE 9: GSTP1 labeling of foveal cones in macula of a 3-year-old monkey. This montage shows strongest labeling by antibody against GSTP1 (red) over the myoid and ellipsoid regions of cones identified by monoclonal antibody 7G6 (green).

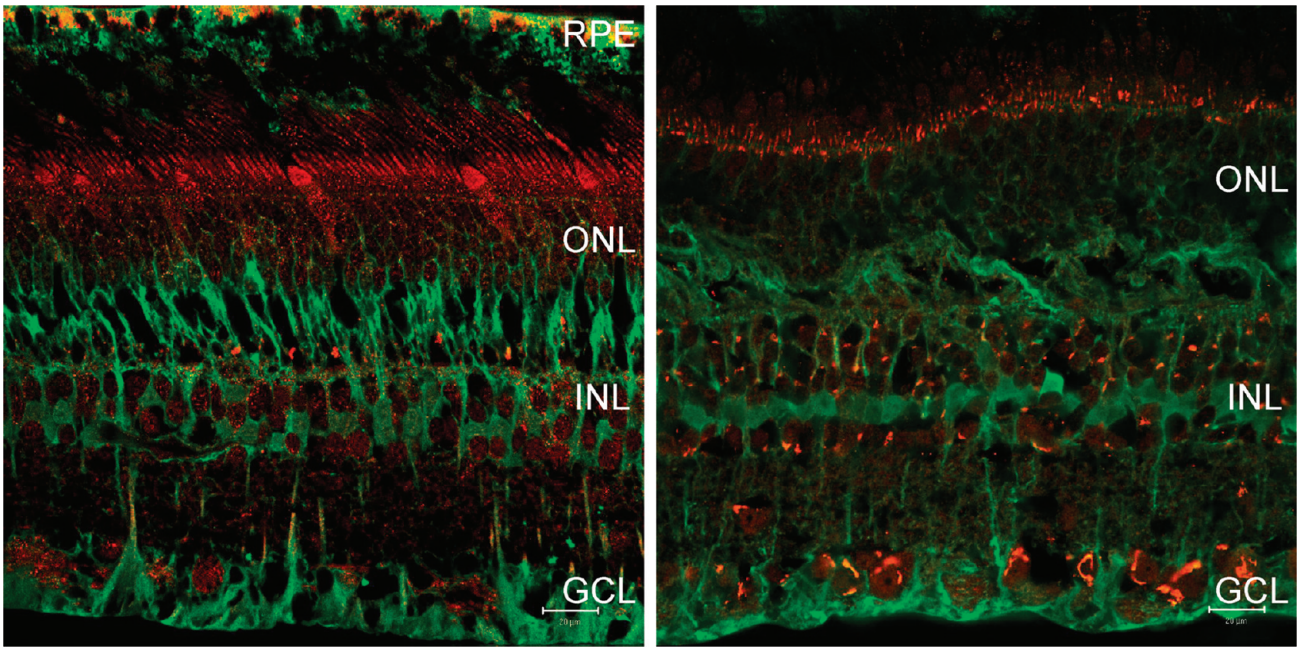

FIGURE 10: Immunolocalization of lutein- and zeaxanthin-binding proteins versus cellular retinaldehyde-binding protein (CRALBP), a marker of Müller glial cells. Left panel: Peripheral region of 9-year-old monkey retina labeled using anti-CBP (red). Stronger CBP immunoreactivity appears over photoreceptor inner segments, with weaker signal associated with neuronal cell bodies of the inner nuclear layer (INL) and ganglion cell layer (GCL). Right panel: Parafoveal region of 3-year-old monkey retina labeled using anti-GSTP1 (red). GSTP1 immunoreactivity is associated with photoreceptor myoid regions and perinuclear locales of neurons of the INL and GCL. Anti-CRALBP (green) labels specifically the retinal pigment epithelium (RPE) and Müller glia and does not colocalize with either xanthophyll-binding protein.

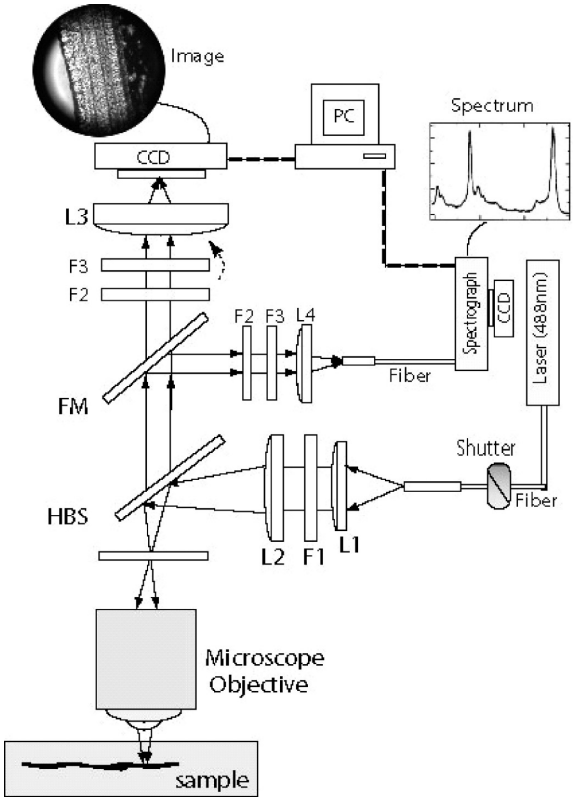

FIGURE 11: Resonance Raman microscope for imaging carotenoid distributions in monkey retinal sections. See Experimental Procedures for details.

and immunohistochemistry with this antibody shows specific localization to the layers of the primate macula where the macular carotenoids are known to be at their highest concentrations. While this may seem surprising at first, this insect protein shares common amino acid sequences with many members of the steroidogenic acute regulatory (StAR) family of mammalian proteins (*33*, *34*, *41*). This group of at least 15 different human proteins is found in diverse tissues where they bind a variety of hydrophobic ligands (*43*). Most notably, the *corpus luteum* of the human ovary, another particularly carotenoid-rich tissue, is known to have abundant StAR1 in its cytoplasm (*51*). Thus, it appears that employment of StAR family proteins to deposit lutein in tissues is a common feature in organisms ranging from insects to humans. The sequence identity of the human retinal lutein-binding protein remains elusive, however. Mass spectral sequencing of the major bands and spots on 1-D and 2-D gels of highly purified HR-LBP has proven unrevealing, a problem occasionally seen when dealing with very hydrophobic proteins. We know that commercial antibodies to two StAR family proteins (StAR1 and MLN64) do not react with HR-LBP, but this leaves at least 13 other StAR family members to be evaluated in the future.

The large bathochromic shift of HR-LBP was not anticipated in our initial attempts to purify xanthophyll-binding proteins from the human retina, especially since the *macula lutea* has maximal absorbance at 460 nm, as we found with zeaxanthin bound to GSTP1. Larger bathochromic shifts may be due to exciton coupling interactions between adjacent chromophores in the binding pocket, a phenomenon well characterized in lobster crustacyanin (*45*). In the fovea, zeaxanthin is the predominant carotenoid, and its protein-bound spectrum dominates the macular pigment's absorption there where optical densities at 460 nm are in the 0.1−1.0 range. In more peripheral areas of the retina, lutein predominates, but since its concentration is 100-fold lower than zeaxanthin in the fovea, it is difficult to record a clear absorption spectrum *in situ* (*18*). Our detection of the first specific lutein-binding protein in the human retina does not, however, rule out the presence of additional lutein-binding proteins

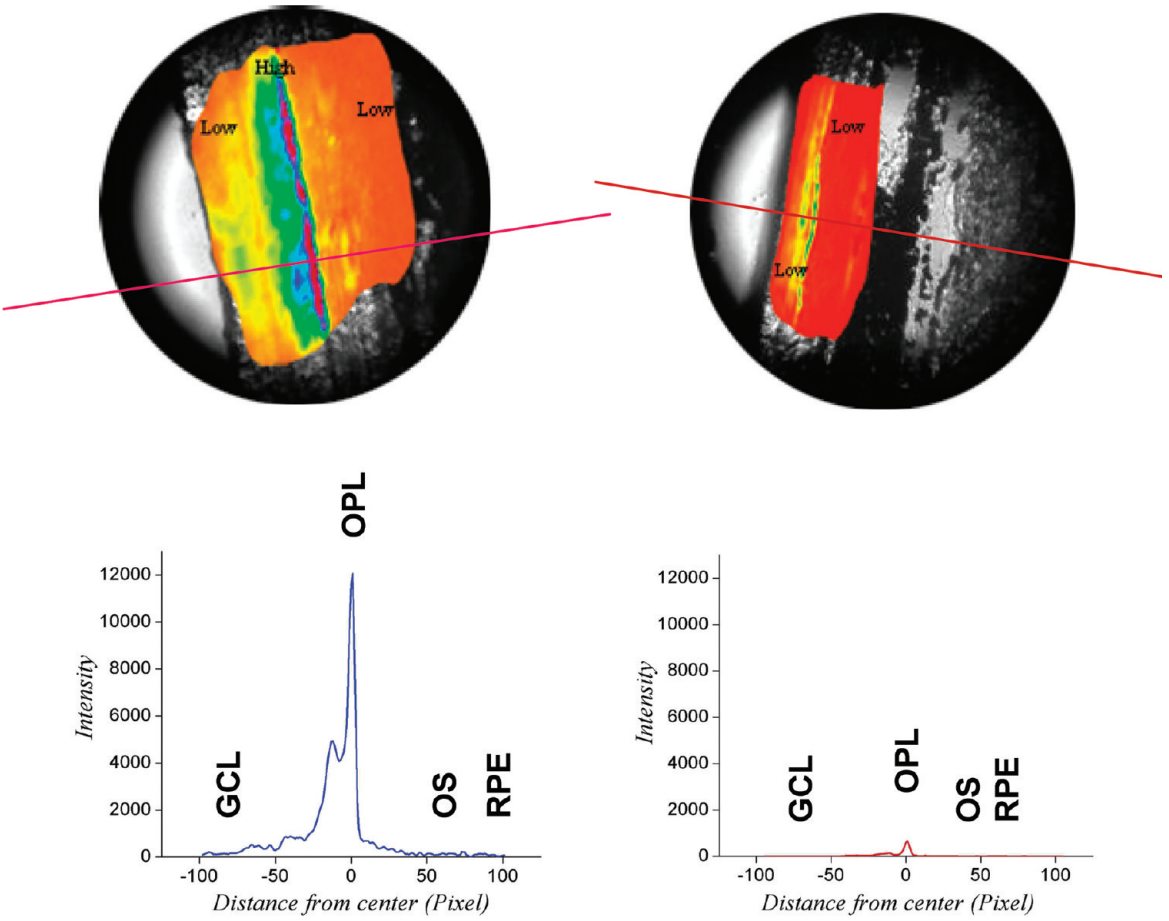

FIGURE 12: Resonance Raman imaging of macular carotenoids. Resonance Raman images of carotenoids in parafoveal (~0.5 mm eccentricity; upper left) and peripheral macular (~3 mm eccentricity; upper right) retina sections from the 9-year-old monkey were made using the resonance Raman microscope shown in Figure 11. Quantitation of Raman intensity along the indicated axes demonstrated that the highest intensity was in the outer plexiform layer (OPL) with very low intensity in the ganglion cell layer (GCL), outer segments, and retinal pigment epithelium (RPE) (lower panels). Raman intensity was generally 100-fold lower in the more peripheral section relative to the parafoveal section.

with absorbance spectra more similar to the foveal macular pigment.

While GSTP1's predominant immunolocalization in the Henle fiber layer of the central macula corresponds well with the distribution of the foveal xanthophylls detected by resonance Raman and absorbance spectroscopy imaging, HR-LBP's apparent immunolocalization predominantly in the photoreceptor ellipsoid region across a wider range of the retina implies that it may play a role other than simply mediating carotenoid deposition in tissues. Since the ellipsoid region is particularly rich in mitochondria, we speculate that HR-LBP may facilitate lutein's antioxidant role in a region of the cell subject to considerable oxidative stress, while GSTP1's intense localization to the fovea's Henle fiber layer suggests zeaxanthin is more likely to serve as a foveal filter for photoxic blue light.

In summary, continued progress in identifying and characterizing new xanthophyll-binding proteins in the human retina should enhance our ability to understand their roles in protecting the macula against light-induced oxidative stress associated with age-related macular degeneration. Our finding that HR-LBP shares many properties with the lutein-binding protein found in the gut and silk gland of the Asian silkworm (*B. mori*) suggests that the xanthophyll-binding protein family performs vital physiological functions in an extraordinarily wide variety of organisms.

ACKNOWLEDGMENT

The Utah Lions Eye Bank generously provided human donor eyes that were critical for completion of this project.

REFERENCES

1. Del Priore, L. V., Tezel, T. H., and Kaplan, H. J. (2006) Maculoplasty for age-related macular degeneration: reengineering Bruch's membrane and the human macula. *Prog. Retinal Eye Res. 25*, 539–562.
2. Alves-Rodrigues, A., and Shao, A. (2004) The science behind lutein. *Toxicol. Lett. 15*, 57–83.
3. Penfold, P. L., Madigan, M. C., Gillies, M. C., and Provis, J. M. (2001) Immunological and aetiological aspects of macular degeneration. *Prog. Retinal Eye Res. 20*, 385–414.
4. Wu, J., Seregard, S., and Algvere, P. V. (2006) Photochemical damage of the retina. *Surv. Ophthalmol. 51*, 461–481.
5. Engel, H. M., Dawson, W. W., Ulshafer, R. J., Hines, M. W., and Kessler, M. J. (1988) Degenerative changes in maculas of rhesus monkeys. *Ophthalmologica 196*, 143–150.
6. Adler, R., Curcio, C., Hicks, D., Price, D., and Wong, F. (1999) Cell death in age-related macular degeneration. *Mol. Vision 3*, 31.
7. Elizabeth Rakoczy, P., Yu, M. J., Nusinowitz, S., Chang, B., and Heckenlively, J. R. (2006) Mouse models of age-related macular degeneration. *Exp. Eye Res. 82*, 741–752.
8. Neuringer, M., Sandstrom, M. M., Johnson, E. J., and Snodderly, D. M. (2004) Nutritional manipulation of primate retinas, I: effects of lutein or zeaxanthin supplements on serum and macular pigment in xanthophyll-free rhesus monkeys. *Invest. Ophthalmol. Visual Sci. 45*, 3234–3243.
9. Thomson, L. R., Toyoda, Y., Delori, F. C., Garnett, K. M., Wong, Z. Y., Nichols, C. R., Cheng, K. M., Craft, N. E., and Dorey, C. K.

(2002) Long term dietary supplementation with zeaxanthin reduces photoreceptor death in light-damaged Japanese quail. *Exp. Eye Res. 75*, 529–542.
10. Khachik, F., de Moura, F. F., Zhao, D. Y., Aebischer, C. P., and Bernstein, P. S. (2002) Transformations of selected carotenoids in plasma, liver, and ocular tissues of humans and in nonprimate animal models. *Invest. Ophthalmol. Visual Sci. 43*, 3383–3392.
11. Bhosale, P., Serban, B., Zhao, D. Y., and Bernstein, P. S. (2007) Identification and metabolic transformations of carotenoids in ocular tissues of the Japanese quail *Coturnix japonica*. *Biochemistry 46*, 9050–9057.
12. Wald, G. (1968) The molecular basis of visual excitation. *Nature 219*, 800–807.
13. Nussbaum, J. J., Pruett, R. C., and Delori, F. C. (1981) Historic perspectives. Macular yellow pigment. The first 200 years. *Retina 1*, 296–310.
14. Bone, R. A., Landrum, J. T., Hime, G. W., Cains, A., and Zamor, J. (1993) Stereochemistry of the human macular carotenoids. *Invest. Ophthalmol. Visual Sci. 34*, 2033–2040.
15. Bhosale, P., Zhao, D. Y., Serban, B., and Bernstein, P. S. (2007) Identification of 3-methoxyzeaxanthin as a novel age-related carotenoid metabolite in the human macula. *Invest. Ophthalmol. Visual Sci. 48*, 1435–1440.
16. Hendrickson, A., Djajadi, H., Erickson, A., and Possin, D. (2006) Development of the human retina in the absence of ganglion cells. *Exp. Eye Res. 83*, 920–931.
17. Snodderly, D. M., Brown, P. K., Delori, F. C., and Auran, J. D. (1984) The macular pigment. I. Absorbance spectra, localization, and discrimination from other yellow pigments in primate retinas. *Invest. Ophthalmol. Visual Sci. 6*, 660–673.
18. Landrum, J. T., and Bone, R. A. (2001) Lutein, zeaxanthin, and the macular pigment. *Arch. Biochem. Biophys. 385*, 28–40.
19. Snodderly, D. M., Auran, J. D., and Delori, F. C. (1984) The macular pigment. II. Spatial distribution in primate retinas. *Invest. Ophthalmol. Visual Sci. 25*, 674–85.
20. Bone, R. A., and Landrum, J. T. (1984) Macular pigment in Henle fiber membranes: a model for Haidinger's brushes. *Vision Res. 24*, 103–108.
21. Bone, R. A., Landrum, J. T., Friedes, L. M., Gomez, C. M., Kilburn, M. D., Menendez, E., Vidal, I., and Wang, W. (1997) Distribution of lutein and zeaxanthin stereoisomers in the human retina. *Exp. Eye Res. 64*, 211–218.
22. Rapp, L. M., Maple, S. S., and Choi, J. H. (2000) Lutein and zeaxanthin concentrations in rod outer segment membranes from perifoveal and peripheral human retina. *Invest. Ophthalmol. Visual Sci. 41*, 1200–1209.
23. Czeczuga-Semeniuk, E., and Wolczynski, S. (2005) Identification of carotenoids in ovarian tissue in women. *Oncol. Rep. 14*, 1385–1392.
24. Snodderly, D. M., Handelman, G. J., and Adler, A. J. (1991) Distribution of individual macular pigment carotenoids in central retina of macaque and squirrel monkeys. *Invest. Ophthalmol. Visual Sci. 32*, 268–279.
25. Trieschmann, M., van Kuijk, F. J., Alexander, R., Hermans, P., Luthert, P., Bird, A. C., and Pauleikhoff, D. (2008) Macular pigment in the human retina: histological evaluation of localization and distribution. *Eye 22*, 132–137.
26. Bhosale, P., Zhao, D,Y., and Bernstein, P. S. (2007) HPLC measurement of ocular carotenoid levels in human donor eyes in the lutein supplementation era. *Invest. Ophthalmol. Visual Sci. 48*, 543–549.
27. Bhosale, P., Larson, A. J., Frederick, J. M., Southwick, K., Thulin, C. D., and Bernstein, P. S. (2004) Identification and characterization of a Pi isoform of glutathione S-transferase (GSTP1) as a zeaxanthin-binding protein in the macula of the human eye. *J. Biol. Chem. 279*, 49447–49454.
28. Bernstein, P. S., Zhao, D. Y., Sharifzadeh, M., Ermakov, I. V., and Gellermann, W. (2004) Resonance Raman measurement of macular carotenoids in the living human eye. *Arch. Biochem. Biophys. 430*, 163–169.
29. Hammond, B. R.Jr., Johnson, E. J., Russell, R. M., Krinsky, N. I., Yeum, K. J., Edwards, R. B., and Snodderly, D. M. (1997) Dietary modification of human macular pigment density. *Invest. Ophthalmol. Visual Sci. 38*, 1795–1801.
30. Trieschmann, M., Beatty, S., Nolan, J. M., Hense, H. W., Heimes, B., Austermann, U., Fobker, M., and Pauleikhoff, D. (2007) Changes in macular pigment optical density and serum concentrations of its constituent carotenoids following supplemental lutein and zeaxanthin: the LUNA study. *Exp. Eye Res. 84*, 718–728.
31. Bassi, R., Pineau, B., Dainese, P., and Marquardt, J. (1993) Carotenoid-binding proteins of photosystem II. *Eur. J. Biochem. 212*, 297–303.
32. Kakitani, Y., Fujii, R., Hayakawa, Y., Kurahashi, M., Koyama, Y., Harada, J., and Shimada, K. (2007) Selective binding of carotenoids with a shorter conjugated chain to the LH2 antenna complex and those with a longer conjugated chain to the reaction center from *Rubrivivax gelatinosus*. *Biochemistry 46*, 7302–7313.
33. Sakudoh, T., Tsuchida, K., and Kataoka, H. (2005) BmStart1, a novel carotenoid-binding protein isoform from *Bombyx mori*, is orthologous to MLN64, a mammalian cholesterol transporter. *Biochem. Biophys. Res. Commun. 336*, 1125–1135.
34. Sakudoh, T., Sezutsu, H., Nakashima, T., Kobayashi, I., Fujimoto, H., Uchino, K., Banno, Y., Iwano, H., Maekawa, H., Tamura, T., Kataoka, H., and Tsuchida, K. (2007) Carotenoid silk coloration is controlled by a carotenoid-binding protein, a product of the Yellow blood gene. *Proc. Natl. Acad. Sci. U.S.A. 104*, 8941–8946.
35. Bhosale, P., and Bernstein, P. S. (2007) Vertebrate and invertebrate carotenoid-binding proteins. *Arch. Biochem. Biophys. 458*, 121–127.
36. Clevidence, B. A., and Bieri, J. G. (1993) Association of carotenoids with human plasma lipoproteins. *Methods Enzymol. 214*, 33–46.
37. During, A., Doraiswamy, S., and Harrison, E. H. (2008) Xanthophylls are preferentially taken up compared with beta-carotene by retinal cells via a SRBI-dependent mechanism. *J. Lipid Res. 49*, 1715–1724.
38. Bernstein, P. S., Balashov, N. A., Tsong, E. D., and Rando, R. R. (1997) Retinal tubulin binds macular carotenoids. *Invest. Ophthalmol. Visual Sci. 38*, 167–175.
39. Matthews, S. J., Ross, N. W., Lall, S. P., and Gill, T. A. (2006) Astaxanthin binding protein in Atlantic salmon. *Comp. Biochem. Physiol., Part B: Biochem. Mol. Biol. 144*, 206–214.
40. Sharifzadeh, M., Zhao, D. Y., Bernstein, P. S., and Gellermann, W. J. (2008) Resonance Raman imaging of macular pigment distributions in the human retina. *J. Opt. Soc. Am. A 25*, 947–957.
41. Tabunoki, H., Sugiyama, H., Tanaka, Y., Fujii, H., Banno, Y., Jouni, Z. E., Kobayashi, M., Sato, R., Maekawa, H., and Tsuchida, K. (2002) Isolation, characterization, and cDNA sequence of a carotenoid binding protein from the silk gland of *Bombyx mori* larvae. *J. Biol. Chem. 277*, 32133–32140.
42. Sierra, A. (2002) Neurosteroids: the StAR protein in the brain. *J. Neuroendocrinol. 16*, 787–793.
43. Alpy, F., and Tomasetto, C. (2005) Give lipids a START: the StAR-related lipid transfer (START) domain in mammals. *J. Cell Sci. 118*, 2791–2801.
44. Gass, J. D. (1999) Müller cell cone, an overlooked part of the anatomy of the fovea centralis: hypotheses concerning its role in the pathogenesis of macular hole and foveomacular retinoschisis. *Arch. Ophthalmol. 117*, 821–823.
45. Zagalsky, P. E. (2003) beta-Crustacyanin, the blue-purple carotenoprotein of lobster carapace: consideration of the bathochromic shift of the protein-bound astaxanthin. *Acta Crystallogr, Sect. D: Biol. Crystallogr. 59*, 1529–1531.
46. Leeson, S., and Caston, L. (2004) Enrichment of eggs with lutein. *Poult. Sci. 83*, 1709–1712.
47. McGraw, K. J., Beebee, M. D., Hill, G. E., and Parker, R. S. (2003) Lutein-based plumage coloration in songbirds is a consequence of selective pigment incorporation into feathers. *Comp. Biochem. Physiol., Part B: Biochem. Mol. Biol. 135*, 689–696.
48. Lakshman, M. R., and Okoh, C. (1993) Enzymatic conversion of all-trans-beta-carotene to retinal. *Methods Enzymol. 214*, 256–269.
49. von Lintig, J., and Vogt, K. (2000) Filling the gap in vitamin A research. Molecular identification of an enzyme cleaving beta-carotene to retinal. *J. Biol. Chem. 275*, 11915–11920.
50. Yemelyanov, A. Y., Katz, N. B., and Bernstein, P. S. (2001) Ligand-binding characterization of xanthophyll carotenoids to solubilized membrane proteins derived from human retina. *Exp. Eye Res. 72*, 381–392.
51. Sierralta, W. D., Kohen, P., Castro, O., Muñoz, A., Strauss, J. F.III, and Devoto, L. (2005) Ultrastructural and biochemical evidence for the presence of mature steroidogenic acute regulatory protein (StAR) in the cytoplasm of human luteal cells. *Mol. Cell. Endocrinol. 242*, 103–110.